第 48 卷第 3 期　　硅　酸　盐　学　报　　Vol. 48，No. 3
2020 年 3 月　　JOURNAL OF THE CHINESE CERAMIC SOCIETY　　March，2020
http://www.gxyb.cbpt.cnki.net　　DOI：10.14062/j.issn.0454-5648.20190446

Sm/Sb 共掺$(Bi_{0.5}Na_{0.5})_{0.935}Ba_{0.065}TiO_3$陶瓷的电致应变与光致发光特性

梁　岑，李　伟，楚丙凯，郝继功，李　伟*

(聊城大学材料科学与工程学院，山东 聊城 252059)

摘　要：介绍了一种无铅发光应变材料$(Bi_{0.5}Na_{0.5})_{0.935-x}Sm_xBa_{0.065}Ti_{1-x}Sb_xO_3$ (BNT–0.065BT–*x*SmSb)陶瓷。研究了 Sm/Sb 对 BNT–0.065BT 相结构、形貌和电性能的影响。BNT–0.065BT–*x*SmSb 陶瓷均呈现纯钙钛矿相结构。Sm/Sb 的加入诱导铁电弛豫相变，从而促进了应变的改善。当 *x*=0.004 时，单极应变为 0.31% (70 kV/cm)，相当于大信号 $d_{33}^*(S_{max}/E_{max})$为 443 pm/V。此外，发光性能研究表明，BNT–0.065BT–*x*SmSb 陶瓷在 407 nm 激发下呈现明亮的橙红色发光。发光强度随着 Sm/Sb 掺杂浓度的增加而增大，其主要发射峰为 599 nm 附近的强红色发射峰，对应于 $^4G_{5/2}\rightarrow{}^6H_{7/2}$ 跃迁。BNT–0.065BT–*x*SmSb 陶瓷作为一种多功能材料，在光电一体化和耦合器件的应用中显示出巨大的潜力。

关键词：无铅陶瓷；电致应变；光致发光
中图分类号：TQ175　　**文献标志码：**A　　**文章编号：**0454–5648(2020)03–0351–05
网络出版时间：2019–12–12

Photoluminescence and Electric-field-induced Strain of Sm/Sb-doped $(Bi_{0.5}Na_{0.5})_{0.935}Ba_{0.065}TiO_3$ Multifunctional Ceramics

LIANG Cen, *LI Wei*, *CHU Bingkai*, *Hao Jigong*, *Li Wei**
(College of Materials Science and Engineering, Liaocheng University, Liaocheng 252059, Shandong, China)

Abstract: In this paper, new lead-free luminescent ferroelectric materials, $(Bi_{0.5}Na_{0.5})_{0.935-x}Sm_xBa_{0.065}Ti_{1-x}Sb_xO_3$ (BNT–0.065BT–*x*SmSb) ceramics, were prepared by introducing Sm/Sb. The influence of Sm/Sb on the phase structure, microstructure and electrical functions of BNT–0.065BT was systematically studied. BNT–0.065BT–*x*SmSb ceramics presented a pure perovskite phase structure. Doping with Sm/Sb induced a ferroelectric to relaxor phase transformation and thus promoted strain improvement. When *x*= 0.004, the unipolar strain was 0.31% (70 kV/cm), equivalent to a large signal $d_{33}^*(S_{max}/E_{max})$ of 443 pm/V. Moreover, studies on the luminescence properties showed that BNT–0.065BT–*x*SmSb ceramics exhibited bright orange-red luminescence under 407 nm excitation. The luminescence intensity increased as the Sm/Sb doping concentration increased. The main emission peak was a strong red emission peak located near 599 nm, corresponding to the $^4G_{5/2}\rightarrow{}^6H_{7/2}$ transition. As multifunctional materials, BNT–0.065BT–*x*SmSb ceramics showed great latent capacity for optical–electrical integration and coupling device applications.

Keywords: lead-free ceramics; electric-field-induced strain; photoluminescence

Introduction

Piezoelectric materials have a wide range of applications in electronics, and the most commonly used materials are piezoelectric materials based on the $PbTiO_3$–$PbZrO_3$ (PZT) system. However, PZT system materials contain large amounts of lead substances that are harmful to the environment and the human body. As

收稿日期：2019–07–01。　修订日期：2019–07–21。
基金项目：国家重点研发计划(2016YFB0402701)；山东省高等学校优秀青年创新团队支持计划(2019KJA025)；聊城大学科研项目(318011906)。
第一作者：梁　岑(1994—)，女，硕士研究生。
通信作者：郝继功(1984—)，男，副教授；
李　伟*(1981—)，男，副教授。

Received date: 2019–07–01.　**Revised date:** 2019–07–21.
First author: LIANG Cen (1994–), female, Master candidate.
E-mail: 515919465@qq.com
Correspondent author: HAO Jigong (1984–), male, Ph.D., associate Professor.
LI Wei* (1981–), male, Ph.D., associate Professor.
E-mail: haojigong@lcu.edu.cn
liwei@lcu.edu.cn

people's awareness of environmental protection increases, lead-based PZT-type materials are gradually replaced by lead-free piezoelectric materials. $Bi_{0.5}Na_{0.5}TiO_3$ (BNT) has a high Curie temperature (T_C=320 ℃) and a high remanent polarization (P_r=38 μC/cm^2)[1–2] and is considered a promising lead-free system. However, pure BNT is difficult to fully polarize due to its large coercive field (E_c=73 kV/cm). Thus, its piezoelectric property is limited, which is an obstacle to the application of BNT[3]. To solve this problem, an appropriate amount of $BaTiO_3$ (BT) is doped into the BNT to form the BNT–BT system. It was found that the BNT–BT binary system formed a morphotropic phase boundary (MPB) when the BT content was 6%–7%, and enhanced piezoelectric properties were obtained[4–6]. In addition, recent studies have found that doping rare earth (RE) elements in the BNT-based system improved the piezoelectric properties. Furthermore, considering the luminescence characteristics of RE ions, photoluminescence (PL) can be realized in BNT-based ceramics.

Similar to PZT-based ceramics, the BNT–BT-based system can obtain a giant electric field-induced strain by introducing minor modifications, such as metal dopants[7–8], $A_2B_2O_6$/ABO_3-type compounds[9–10], or *B*-site complex ion substitution[11–12]. When these additives contain RE elements, the modified ceramics can exhibit luminescent properties. However, most studies concern single RE element doping for fabricating multifunctional BNT-based ceramics[13–16]. A few studies concern *B*-site complex ion substitution in BNT–BT to obtain multifunctional piezoelectric ceramics. For example, Hao et al. [11] achieved a large strain of 0.40% and green emission in Er/Sb-modified BNT–6.5BT ceramics. Therefore, in the present work, an RE element Sm and a metal element Sb are introduced in BNT–0.065BT to achieve a large strain response and luminescence effect by forming a solid solution $(Bi_{0.5}Na_{0.5})_{0.935-x}Sm_xBa_{0.065}Ti_{1-x}Sb_xO_3$.

1 Experimental

In this experiment, $(Bi_{0.5}Na_{0.5})_{0.935-x}Sm_xBa_{0.065}Ti_{1-x}Sb_xO_3$ ceramic samples are prepared by the conventional solid phase reaction method. The raw materials are Na_2CO_3 (99.8%), Bi_2O_3 (99.8%), $BaCO_3$ (99%), TiO_2 (99.5%), and Sm_2O_3 (99.9%) from Sinopharm Chemical Reagent, China, and Sb_2O_3 (99%) from Tianjin Damao, China. First, the required raw materials are weighed according to the stoichiometric ratio and then placed in a ball mill pot and milled for 15 h. The dried powders are pressed into a large piece with a diameter of 25 mm. After calcining the powder at 850 ℃, the calcined powders are then ball milled again for 15 h. Polyvinyl alcohol (PVA) solution is then added to the ceramic powder for granulation, which is advantageous for subsequent dry pressing. Sintering is carried out after pressing several ceramic sheets, and the sintering temperature of this experiment is 1 120 ℃. The sintered ceramic sheets are left for XRD, SEM and luminescence testing, and another portion is pasted to silver electrodes for subsequent electrical performance testing.

We used X-ray diffraction (XRD, Bruker D8 Advance, Germany) to analyze the crystal structure of the ceramics. Electrical field–related parameters, including polarization hysteresis (*P*–*E*), bipolar strain (*S*–*E*) and unipolar strain (*S*–*E*), were measured by a ferroelectric analyzer (aix–ACCT Inc., Germany). We analyzed the photoluminescence (PL) and PL excitation (PLE) properties using a spectrofluorometer (FLS920, Edinburgh Instruments, UK).

2 Result and discussion

Fig. 1 shows the XRD pattern of BNT–0.065BT–*x*SmSb ceramics in the range of 20°–70°. All ceramics show a pure perovskite phase, indicating that Sm/Sb ions completely enter into the BNT–0.065BT ceramics to form a uniform solid solution. Note that no obvious split peaks are observed in Fig. 1, indicating that all BNT–0.065BT–*x*SmSb ceramics have a pseudocubic structure[17]. Although there are no noncubic distortions, it can be assumed that the symmetry of the ceramic on the local scale should be less than cubic, and its dimension exceeds the detection limit of conventional X-ray diffraction techniques[18]. Furthermore, according to previous reports[19–21], BNT–BT-based nanocrystals have pseudosymmetric rhombohedral and tetragonal polar nanocrystals (PNRs). The small amount of Sm/Sb doping does not cause a significant change in the phase structure of BNT–0.065BT.

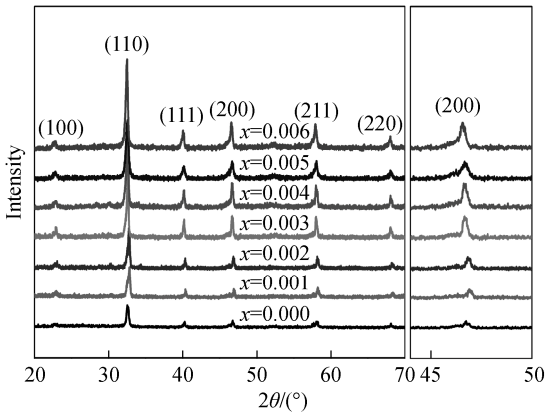


Fig. 1 XRD pattern of BNT–0.065BT–*x*SmSb ceramics

Fig. 2(a)–Fig. 2(g) shows the surface micrograph of BNT–0.065BT–*x*SmSb ceramics. The SEM images show that all ceramics are dense and uniform during sintering. The ceramics are compared with pure BNT–0.065BT ceramics, this can be seen from Fig. 2(h) that, the grain sizes of Sm/Sb-doped ceramics decrease with increases of the doping amount, indicating that Sm/Sb can exist as a growth inhibitor in BNT–0.065BT–*x*SmSb ceramics. However, there is no obvious morphological change.

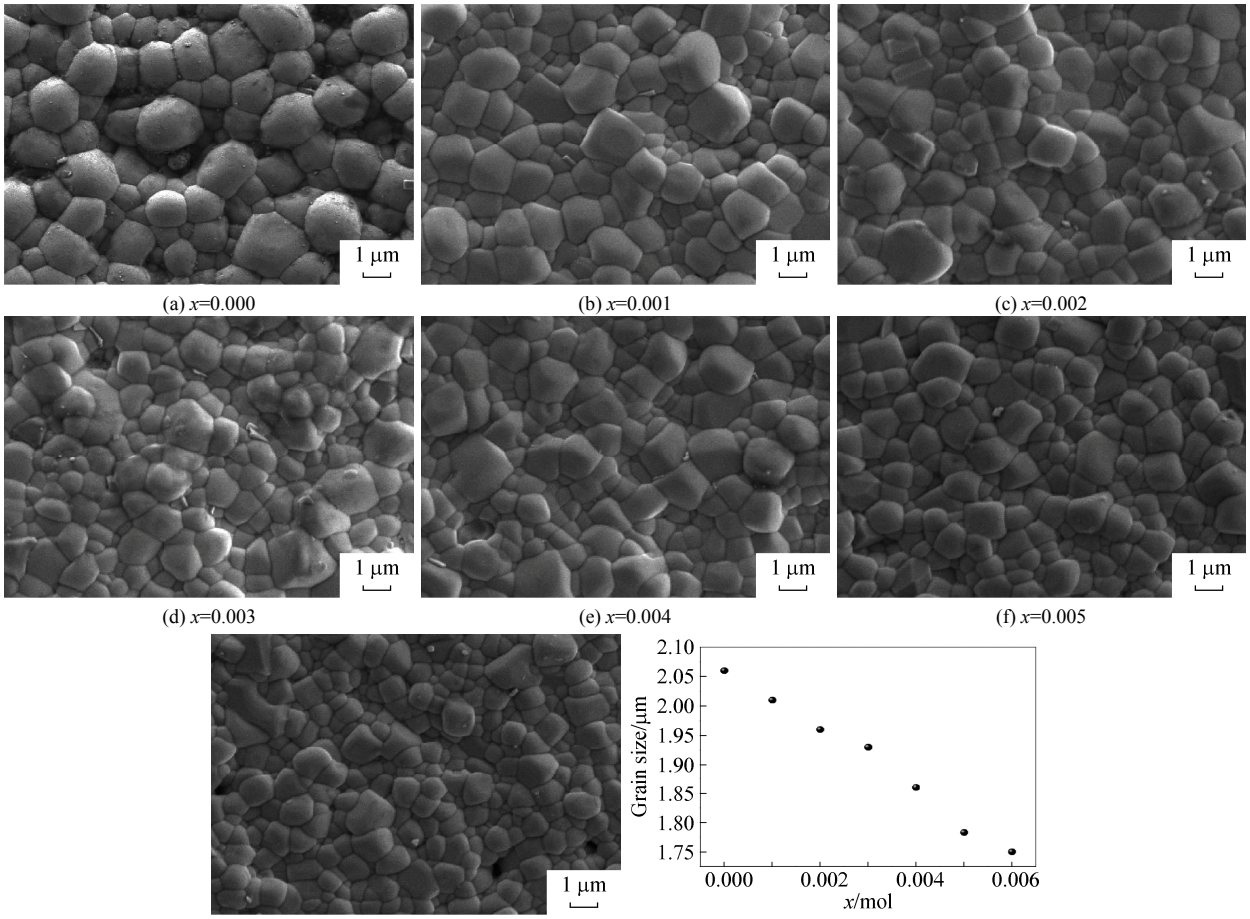


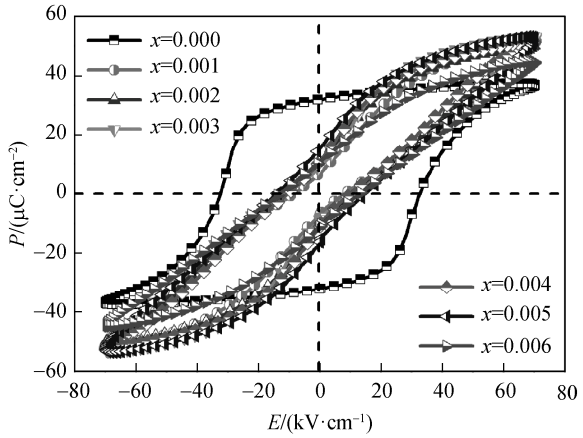
Fig. 2　Surface micrograph of BNT–0.065BT–*x*SmSb ceramics

Fig. 3 shows the hysteresis loops and *I*–*E* curves of BNT–0.065BT–*x*SmSb ceramics measured at 10 Hz and room temperature, respectively. The saturated square hysteresis loop appears in pure BNT–0.065BT ceramic, and there is only one peak current (P_1) near the coercive field (E_c). Meanwhile, the pure BNT–0.065BT ceramic has a large P_r of 32 μC/cm^2 and high E_c of 32 kV/cm, which confirms that pure BNT–0.065BT ceramic is typical of long-range ordered ferroelectrics. As the amount of Sm/Sb dopants increases, both P_r and E_c are greatly reduced, and the hysteresis loops become narrower and show a "pinched" shape. At the same time, in Fig. 3(b), it can be seen that the *I*–*E* curves in the Sm/Sb-doped samples show another P_2-peak in addition to the P_1-peak. The results show that the incorporation of Sm/Sb interferes with the long-range ferroelectric order of BNT–0.065BT ceramics, which induces the ergodic relaxor state at zero field in modified BNT–0.065BT ceramics with the addition of an electric field; the ergodic relaxor state reversibly transforms to a ferroelectric state[17] and thus generally results in a large electric-field-induced strain response.

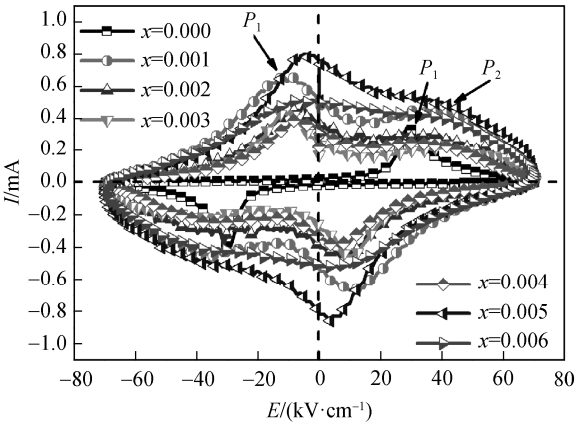
The bipolar strain curves shown in Fig. 4(a) also indicate that BNT–0.065BT–*x*SmSb ceramics have ergodic relaxation characteristics. Since pure BNT–0.065BT is a classical ferroelectric, as discussed above, it exhibits a "butterfly" shaped bipolar strain curve with a large negative strain S_{neg} in the curve. When Sm/Sb is doped into BNT–0.065BT, a "bud" shaped strain curve appears, in which the S_{neg} reduces to zero, and the positive strain S_{pos} significantly increases. The changes in the bipolar strain curves of the Sm/Sb–modified samples also indicate a drastic increase in the unipolar strain (S_{uni}), as shown in Fig. 4(b). Consistent with the change of the bipolar strain curve, the unipolar strain curve in the pure BNT–0.065BT ceramic increases almost linearly with the increase of the electric field, and the hysteresis is low, confirming the typical ferroelectric nature. The strain curves of Sm/Sb-doped BNT–0.065BT–*x*SmSb ceramics have obvious hysteresis, showing ergodic relaxation characteristics. Moreover, it can be seen from the figure that S_{uni} increases with the Sm/Sb dopant amount, and at x=0.004, the unipolar strain value reaches a maximum of 0.31% (at 70 kV/cm) along with a large signal piezoelectric d_{33}^* constant (=S_{max}/E_{max}) of 443 pm/V.

Since the studied BNT–0.065BT–*x*SmSb composition contains Sm, BNT–0.065BT–0.006SmSb ceramics also have excellent luminescent properties. Fig. 5(a) shows the photoluminescence excitation (PLE) at 597 nm and photoluminescence (PL) at 407 nm spectra of BNT–0.065BT–0.006SmSb ceramics. In the PLE

spectrum, two excitation peaks appear in the 375–500 nm interval, one strong excitation peak at 407 nm corresponds to the $^6H_{5/2}\rightarrow{}^4G_{7/2}$ transition, and the other excitation weak peak at 427 nm corresponds to the $^6H_{5/2}\rightarrow{}^4P_{5/2}$ transition[22–23]. Under the 407 nm excitation, three distinct peaks in the PL spectrum are observed: the $^4G_{5/2}\rightarrow{}^6H_{5/2}$ transition at 564 nm, the $^4G_{5/2}\rightarrow{}^6H_{7/2}$ transition at 599 nm, and the $^4G_{5/2}\rightarrow{}^6H_{9/2}$ transition at 646 nm. The above transitions can be seen more clearly in the energy level transitions of Sm^{3+} in Fig. 5(b).



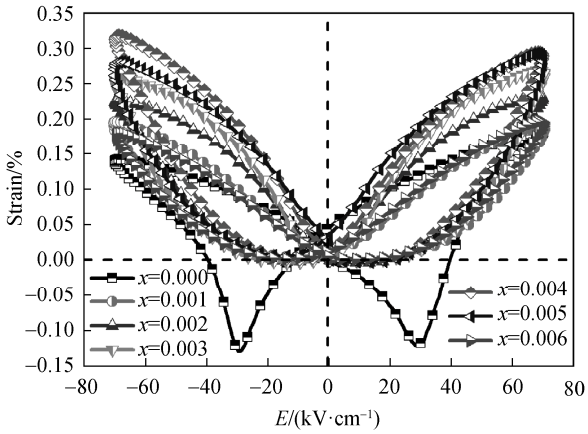
(a) *P–E* hysteresis loop



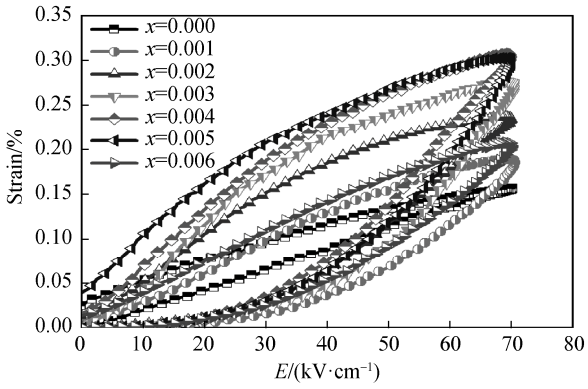
(b) *I–E* curve

Fig. 3 *P–E* hysteresis loops and *I–E* curves of BNT–0.065BT–*x*SmSb ceramics

The PL spectra of BNT–0.065BT–*x*SmSb ceramics with different Sm/Sb contents are shown in Fig. 6(a). It can be seen from the figure that the luminescence intensity increases with the increase of the Sm/Sb doping amount, and the luminescence intensity is maximum at x=0.006. In addition, the positions of the emission peaks in the PL spectra do not shift as the amount of Sm/Sb doping increases. Fig. 6(b) shows a color coordinate (CIE) chart of BNT–0.065BT–*x*SmSb ceramics. The CIEs of all samples are basically at x=0.59 and y=0.44, and coordinate points are in the bright orange-red region, corresponding to the PL spectra. All ceramics show a bright orange red at 407 nm.

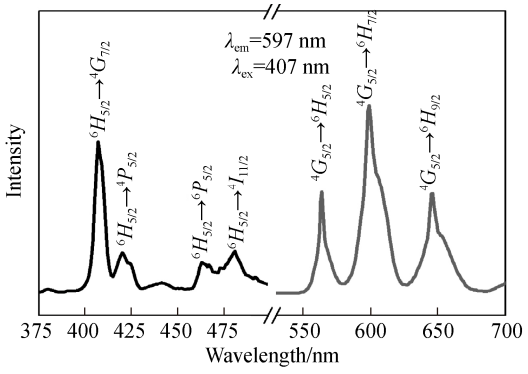


(a) Bipolar strain curve

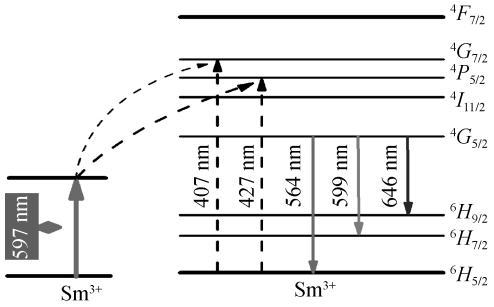


(b) Unipolar strain curve

Fig. 4 Bipolar strain curves and unipolar strain curves of BNT–0.065BT–*x*SmSb ceramics

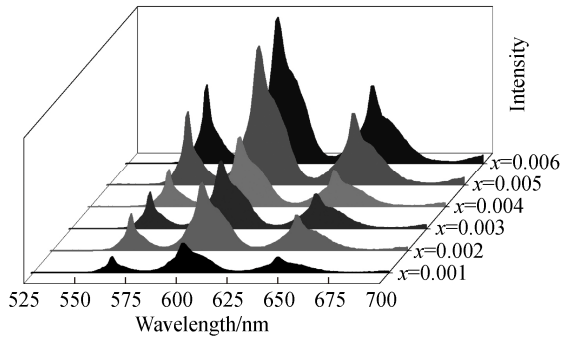


(a) PLE and PL spectra

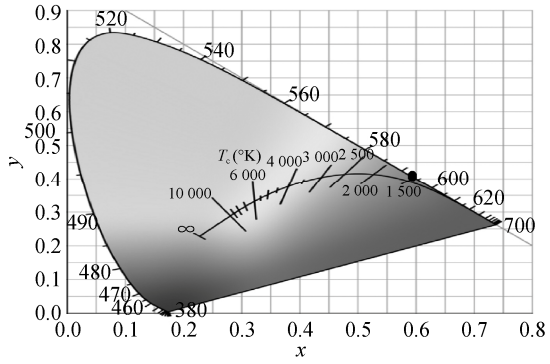


(b) Energy level diagram

Fig. 5 PLE (λ_{em}=597 nm) and PL (λ_{ex}=407 nm) spectra of BNT–0.065BT–0.006SmSb and energy level diagram of Sm^{3+} ions



(a) PL spectra



(b) CIE chromaticity coordinate

Fig. 6　Dependence of PL spectra intensity on Sm/Sb concentrations excited at 407 nm and calculated CIE chromaticity coordinate of BNT–0.065BT–*x*SmSb ceramics

3　Conclusions

BNT–0.065BT–*x*SmSb ceramics were prepared by the solid phase reaction method. All modified ceramics formed a perovskite structure and exhibited characteristics of ergodic relaxor phases. The maximum strain response was 0.31% (d_{33}^* is 443 pm/V) when the doping amount was 0.004. In addition, all ceramics had orange–red luminescence properties at a 407 nm light excitation.

参考文献:

[1] TAKENAKA T, NAGATA H. Present status of non-lead-based piezoelectric ceramics[J]. Key Eng Mater, 1999, 157–158:57–64.

[2] 商鑫亭, 艾彩娇, 顾雅欣, 等. 烧结气氛对BNT–BKT–ST薄膜结构和性能影响[J]. 聊城大学学报(自然科学版), 2018(3): 19–23.
SHANG X, Ai C, GU Y, et al. J Liaocheng Univ:Nat Sci Ed (In Chinese), 2018(3): 19–23.

[3] HERABUT A, SAFARI A. Processing and electromechanical properties of $(Bi_{0.5}Na_{0.5})_{(1-1.5x)}La_xTiO_3$ ceramics[J]. J Am Ceram Soc, 1997, 80(11): 2954–2958.

[4] ZHANG Q, SUN H, WANG X, et al. Highly efficient orange emission $(K_{0.5}Na_{0.5})NbO_3$: Sm^{3+} lead free piezoceramics[J]. Mater Lett, 2014, 117: 283–285.

[5] HAO J, LI W, ZHAI J, et al. Progress in high–strain perovskite piezoelectric ceramics[J]. Mater Sci Eng: R: Reports, 2019, 135: 1–57.

[6] LIANG C, HAO J, LI W, et al. Strong red emission and enhanced electrostrain in $(Bi_{0.5}Na_{0.5})_{0.935-x}Pr_xBa_{0.065}Ti_{1-x}Sb_xO_3$ lead-free multifunctional ceramics[J]. J Mater Sci: Mater Electr, 2018, 29(16): 13810–13817.

[7] HAO J, XU Z, CHU R, et al. Structure evolution and electrostrictive properties in $(Bi_{0.5}Na_{0.5})_{0.94}Ba_{0.06}TiO_3$–$M_2O_5$(M= Nb, Ta, Sb) lead-free piezoceramics[J]. J Eur Ceram Soc, 2016, 36(16): 4003–4014.

[8] YAO Q, WANG F, XU F, et al. Electric field-induced giant strain and photoluminescence–enhancement effect in rare-earth modified lead-free piezoelectric ceramics[J]. ACS Appl Mater Int, 2015, 7(9): 5066–5075.

[9] SHI J, FAN H, LIU X, et al. Giant strain response and structure evolution in $(Bi_{0.5}Na_{0.5})_{0.945-x}(Bi_{0.2}Sr_{0.7})_xBa_{0.055}TiO_3$ ceramics[J]. J Eur Ceram Soc, 2014, 34(15): 3675–3683.

[10] CHENG R, XU Z, CHU R, et al. Microstructure and electrical properties of $Bi_{1/2}Na_{1/2}TiO_3$–$BaTiO_3$–Y_2NiMnO_6 lead-free piezoelectric ceramics[J]. Ceram Inter, 2015, 41(5): 6424–6431.

[11] HAO J, XU Z, CHU R, et al. Bright upconversion emission and large strain in Er/Sb-codoped $(Bi_{0.5}Na_{0.5})_{0.945}Ba_{0.065}TiO_3$ ceramics[J]. Mater Lett, 2017, 193: 138–141.

[12] LI P, LIU B, SHEN B, et al. Large strain response in $Bi_4Ti_3O_{12}$ modified BNT–BT piezoelectric ceramics[J]. Ceram Inter, 2017, 43(1): 1008–1013.

[13] XIA X, JIANG X, CHEN C, et al. Enhanced piezoelectric performance and orange-red emission of Sm^{3+} doped $(Na_{1/2}Bi_{1/2})$ TiO_3 based lead-free ceramics[J]. Ceram Inter, 2017, 43(1): 376–384.

[14] HAO J, XU Z, CHU R, et al. Large electrostrictive effect and strong photoluminescence in rare-earth modified lead-free $(Bi_{0.5}Na_{0.5})TiO_3$-based piezoelectric ceramics[J]. Scripta Mater, 2016, 122: 10–13.

[15] HU B, PAN Z, DAI M, et al. Photoluminescence and temperature dependent electrical properties of Er-doped $0.94Bi_{0.5}Na_{0.5}TiO_3$–$0.06BaTiO_3$ ceramics[J]. J Am Ceram Soc, 2014, 97(12): 3877–3882.

[16] SUN H, WU X, PENG D F, et al. Room-temperature large and reversible modulation of photoluminescence by in situ electric field in ergodic relaxor ferroelectrics[J]. ACS Appl Mater Interf, 2017, 9(39): 34042–34049.

[17] ULLAH A, ALAM M, ULLAH A, et al. High strain response in ternary $Bi_{0.5}Na_{0.5}TiO_3$–$BaTiO_3$–$Bi(Mn_{0.5}Ti_{0.5})O_3$ solid solutions[J]. RSC Adv, 2016, 6(68): 63915–63921.

[18] WANG K, HUSSAIN A, JO W, et al. Temperature-dependent properties of $(Bi_{1/2}Na_{1/2})TiO_3$–$(Bi_{1/2}K_{1/2})TiO_3$–$SrTiO_3$ lead-free piezoceramics[J]. J Am Ceram Soc, 2012, 95(7): 2241–2247.

[19] ZHANG S T, KOUNGA A B, AULBACH E, et al. Giant strain in lead-free piezoceramics $Bi_{0.5}Na_{0.5}TiO_3$–$BaTiO_3$–$K_{0.5}Na_{0.5}NbO_3$ system[J]. Appl Phys Lett, 2007, 91(11): 112906.

[20] JO W, DITTMER R, ACOSTA M, et al. Giant electric–field–induced strains in lead-free ceramics for actuator applications-status and perspective[J]. J Electroceram, 2012, 29(1): 71–93.

[21] GONG Y, HE X, CHEN C, et al. Large electric field-induced strain in ternary $Bi_{0.5}Na_{0.5}TiO_3$–$BaTiO_3$–Sr_2MnSbO_6 lead-free ceramics[J]. Ceram Inter, 2019, 45(6): 7173–7179.

[22] ZHANG Q, ZHANG Y, SUN H, et al. Photoluminescence, photochromism, and reversible luminescence modulation behavior of Sm-doped $Na_{0.5}Bi_{2.5}Nb_2O_9$ ferroelectrics[J]. J Eur Ceram Soc, 2017, 37(3): 955–966.

[23] HAO J, XU Z, CHU R, et al. Bright reddish-orange emission and good piezoelectric properties of Sm_2O_3-modified $(K_{0.5}Na_{0.5})NbO_3$-based lead-free piezoelectric ceramics[J]. J Appl Phys, 2015, 117(19): 194104.